On the use of small-scale results for the design of ventilation systems in large-scale atria

Tilley, N., Rauwoens, P. and Merci, B.

In: Proceedings of the 6th International Seminar on Fire and Explosion Hazards, Leeds, UK, pp. 173-184, 2010.

On the use of small-scale results for the design of ventilation systems in large-scale atria

Tilley, N.*, Rauwoens, P. and Merci, B.

Ghent University – UGent, Department of Flow, Heat and Combustion Mechanics, Sint-Pietersnieuwstraat 41, B-9000 Ghent, Belgium
**Corresponding author email: Nele.Tilley@UGent.be*

ABSTRACT

Many researchers use a set of small-scale atrium experiments to develop formulae for smoke and heat exhaust ventilation systems. They correspond to large-scale atria via Froude-scaling. A similar study can be performed with numerical simulations, where a small-scale setup can be scaled up to compare the results. However, with numerical simulations as well as in experiments, proper scaling is necessary. This paper discusses the dimensionless numbers for scaling. The simulations confirm that scaling based on Froude-number alone seems allowed as long as the flows in all configurations are sufficiently turbulent.

KEYWORDS: *scaling; numerical simulations; smoke extraction; atria*

NOMENCLATURE LISTING

c_p	specific heat capacity (J/(kg.K))	S	rate of strain (1/s)
D	mass diffusivity (m^2/s)	t	time (s)
D_h	hydraulic diameter (m)	T	temperature (K)
f	external force (N)	u	velocity (m/s)
g	gravity acceleration (m/s^2)	W	atrium width (m)
h	enthalpy (J/kg)	Y	mass fraction (-)
H	atrium height (m)	z_s	smoke free height (m)
k	thermal conductivity (W/(m.K))	**Greek**	
L	length (m)	α	thermal diffusivity (m^2/s)
m	mass (kg)	Δ	grid cell size (m)
$\dot{m}$	mass flow rate (kg/s)	μ	dynamic viscosity (Pa.s)
M	mass flow rate (kg/s)	ν	kinematic viscosity (m^2/s)
p	pressure (Pa)	ρ	density (kg/m^3)
$\dot{Q}$	total heat release rate (kW)	τ	stress tensor (Pa)

INTRODUCTION

Atria are a commonly encountered architectural type of buildings. They are often found in shopping malls, hotels and office buildings. When fire occurs in an adjacent room to the atrium, a smoke plume emerges, spills into the atrium and rises to the ceiling of the atrium, to form a smoke layer underneath (Fig. 1).

A smoke and heat exhaust ventilation system can be designed in the atrium to extract smoke at ceiling level, maintaining a certain smoke free height underneath the smoke layer. In the past, several authors [1-8] developed formulae to calculate the required smoke mass flow rate ($M(z_s)$) to be extracted at the ceiling of the atrium, in order to ensure a certain smoke free height (z_s) above the spill edge. The fire heat release rate ($\dot{Q}$) and a length scale parameter of the atrium (a width W) appear in all these formulae.

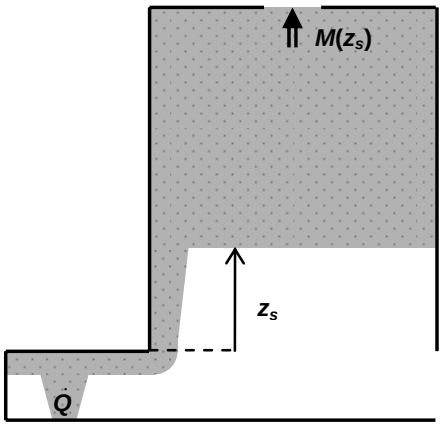

Figure 1. Atrium configuration.

Often, these developed formulae rely on (a large set of) small-scale experiments. Being less expensive, safer to control and easier to handle for a parameter variation study, and requiring less space, small-scale experiments are indeed usually preferred over large-scale experiments. However, for small-scale data formulae to be used in large-scale configurations, proper scaling must be applied. It is commonly assumed that – as long as the flow is sufficiently turbulent – scaling based on Froude number is sufficient in fire problems. This assumption is also used in the above derivation of formulae based on small-scale experiments.

With CFD (Computational Fluid Dynamics) calculations, a parameter variation in large-scale configurations is easier. One could perform simulations for a set of small-scale experiments and afterwards scale up the configuration to check whether the developed formula is still valid in the large-scale setup. However, also with CFD simulations, scaling must be done in a proper way. This is discussed in the present paper.

GOVERNING EQUATIONS – SCALING LAWS

In the present paper, we use FDS (Fire Dynamics Simulator, version 5.2.5 [9]) as CFD code. Therefore the governing equations are written as in the FDS manual. However, conclusions on dimensionless numbers are valid for the equations to be solved in any CFD program.

The three basic governing flow equations (conservation of mass and momentum, and transport of sensible enthalpy), in their instantaneous form, serve as starting point. The important dimensionless numbers and scaling of terms are derived. Such studies have

already been reported (e.g. [10-12]). We repeat the most important features here, as they are relevant in the discussion of the results.

Instantaneous equations and dimensionless numbers

Conservation of mass

$$\frac{\partial \rho}{\partial t} + \nabla \cdot \rho \boldsymbol{u} = \dot{m}_b'' \tag{1}$$

Stating that $\frac{\rho}{t} \sim \frac{\rho u}{L} \sim \frac{m}{L^3 t}$ implies:

$$t \sim L/u \,. \tag{2}$$

In time-dependent scaled simulations, it is important to use this scaling factor to compare instantaneous flow fields at corresponding times.

Conservation of momentum

$$\frac{\partial}{\partial t}\left(\rho \boldsymbol{u}\right) + \nabla \cdot \rho \boldsymbol{u}\boldsymbol{u} + \nabla p = \rho \boldsymbol{g} + \boldsymbol{f}_b + \nabla \cdot \tau_{ij} \tag{3}$$

$$\text{with } \tau_{ij} = \mu\left(2\boldsymbol{S}_{ij} - \frac{2}{3}\delta_{ij}\left(\nabla \cdot \boldsymbol{u}\right)\right), S_{ij} = \frac{1}{2}\left(\frac{\partial u_i}{\partial x_j} + \frac{\partial u_j}{\partial x_i}\right) \tag{4}$$

Equation (3) reveals that $\frac{\rho u}{t} \sim \frac{\rho u^2}{L} \sim \frac{p}{L} \sim \rho g \sim f \sim \mu \frac{u}{L^2}$, resulting in three important dimensionless numbers:

- The Froude number, comparing inertia and gravitational forces, which is important in natural convection: $\mathrm{Fr} = u\rho/\sqrt{gL\Delta\rho}$.

  Maintaining temperatures equal in original and scaled simulations, the Froude number can be simplified. We will use this definition:

$$\mathrm{Fr} = \frac{u}{\sqrt{gL}} \,. \tag{5}$$

- The Reynolds number, comparing inertia and viscous forces, which is important in forced convection:

$$\mathrm{Re} = \frac{uL}{\nu} . \tag{6}$$

- The Euler number, relating a pressure difference to the kinetic energy. We do not consider this number further in the paper, as pressure differences are not relevant here (forced mechanical ventilation with known flow rates).

$$\mathrm{Eu} = \frac{\Delta p}{\rho u^2} . \tag{7}$$

Transport of sensible enthalpy

$$\frac{\partial}{\partial t}\left(\rho h_s\right) + \nabla \cdot \rho h_s \boldsymbol{u} = \frac{Dp}{Dt} + \dot{Q}''' - \dot{Q}_b''' - \nabla \cdot \dot{\boldsymbol{Q}}'' + \tau_{ij} \nabla \boldsymbol{u} \tag{8}$$

$$\text{With } \dot{\boldsymbol{Q}}'' = -k\nabla T - \sum_a h_{s,a} \rho D_a \nabla Y_a + \dot{\boldsymbol{Q}}_r'' \tag{9}$$

$$h_s = \sum_a Y_a h_{s,a} = \sum_a \left(Y_a \int_{T_0}^{T} c_{p,a} T' dT' \right) \tag{10}$$

$$\frac{\rho c_p T}{t} \sim \frac{\rho c_p T u}{L} \sim \frac{p}{t} \sim \frac{\dot{Q}}{L^3} \sim \frac{kT}{L^2} \sim \frac{\rho c_p T D}{L^2} \sim \mu \frac{u^2}{L^2}$$

From transport of sensible enthalpy, the velocity scales as

$$u \sim \frac{\dot{Q}}{L^2 \rho c_p \Delta T} . \tag{11}$$

The Eckert number relates kinetic energy to temperature variations and becomes important only for high-velocity flows (so that it is not relevant for the sake of the study in the present paper):

$$\mathrm{Ec} = \frac{u^2}{c_p \Delta T} . \tag{12}$$

The ratio of kinematic viscosity (or ‘momentum’ diffusivity) and thermal diffusivity is the Prandtl number:

$$\mathrm{Pr} = \frac{\nu}{\alpha} . \tag{13}$$

Similarly, the Schmidt number expresses the ratio of momentum diffusivity and mass diffusivity:

$$\mathrm{Sc} = \frac{\nu}{D}. \tag{14}$$

A final important dimensionless number is the Rayleigh number, a combination of Re, Pr and Fr. The Rayleigh number, for natural convection, is:

$$\mathrm{Ra} = \frac{\mathrm{Re}^2\,\mathrm{Pr}}{\mathrm{Fr}^2} = g\frac{L^3}{\nu\alpha}\frac{\Delta\rho}{\rho}. \tag{15}$$

Influence of numerics and modeling

The standard Smagorinsky turbulence model is used by default in FDS. In this model, a turbulent viscosity is defined as:

$$\nu_T = \left(C_s\Delta\right)^2\left(2\bar{\boldsymbol{S}}_{ij}\bar{\boldsymbol{S}}_{ij} - \frac{2}{3}\left(\nabla\cdot\bar{\boldsymbol{u}}\right)^2\right)^{1/2}, \tag{16}$$

with Δ the grid cell size. It is interesting to note that this turbulent viscosity globally scales as:

$$\nu_T \sim \left(\frac{\Delta}{L}\right)^2 uL. \tag{17}$$

When the ratio Δ/L goes to 0, the turbulent viscosity decreases and the simulation in principle evolves into a DNS simulation.

If the cell size scales proportional to the configuration dimensions, the ratio Δ/L is constant. In this way, the number of cells in the configuration does not change in scaling. The turbulent viscosity then scales as

$$\nu_T \sim uL. \tag{18}$$

An “effective” Reynolds number [13] can be defined, based on the “effective viscosity” (i.e. the sum of the molecular and turbulent viscosities). When the turbulent viscosity is high, relative to the molecular viscosity, the latter can be neglected:

$$\nu_{eff} = \nu + \nu_T \approx \nu_T. \tag{19}$$

The effective Reynolds number then becomes:

$$\mathrm{Re}_{eff} = \frac{uL}{\nu_{eff}} \approx \frac{uL}{\nu_T} = \mathrm{Re}_T \,. \tag{20}$$

Hence, Eq. 18 reveals that with the Smagorinsky LES turbulence model, the effective Reynolds number, which is relevant for forced convection, is automatically preserved in the simulations, regardless of the scaling applied. From the above derivation, it is clear that this is only valid when the turbulent viscosity is sufficiently high relative to the molecular viscosity, i.e. when the flow is sufficiently turbulent.

In the same spirit, a turbulent Rayleigh number can be defined, and reformed with Eq. 18 and Eq. 13 to obtain:

$$\mathrm{Ra}_T = g\frac{L^3}{\alpha\nu_T}\frac{\Delta\rho}{\rho} = \frac{\mathrm{Pr}_T}{\mathrm{Fr}^2}\frac{\Delta\rho}{\rho}\,. \tag{21}$$

Hence, when preserving the Froude number in scaling a configuration and maintaining temperatures equal in original and scaled simulations (see below), the turbulent Rayleigh number (for natural convection) will also be preserved automatically.

Scaling of experiments

When scaling up experimental configurations, obviously no modeling effects need to be taken into account. In experimental test cases, the results are what they are and are by definition according to reality.

However, it is important not to forget about the physics of scaling when dealing with experiments. Especially the difference between laminar and turbulent flow is very important. Indeed, there is a danger that a laminar, or weakly turbulent, small-scale experiment is scaled up, via the Froude-number, to a strongly turbulent large-scale configuration. In this case, the two configurations need not give similar results.

As long as the experimental setup has a turbulent flow behavior (Reynolds and Rayleigh numbers are high, say $\mathrm{Re} > 10^4$ and $\mathrm{Ra} > 10^9$), a scaled up (or down) configuration where both numbers are still sufficiently high, will show the same behavior as the small one.

As shown above, this remains true in numerical modeling, where the turbulent viscosity is so high, compared to the molecular viscosity, that Re and Ra are automatically preserved when scaling with Froude.

RESULTS

Setup of simulations

A number of CFD simulations were run to investigate the effects of scaling. The Froude number is always preserved. The configuration of the simulations was derived from the experiments of Poreh [8].

Atria of W = 0.9 m wide (as in the experimental results of [8]) and 7.2 m wide (exactly the same configuration, only eight times larger spatial dimensions) were simulated. A scaling factor of 8 was chosen here, so that the scaled heat release rate for the new configuration is realistic for fire in an atrium [14]. The atrium height is H = 3.6 m (or H = 28.8 m). We use the hydraulic diameter (D_h), defined as four times the floor area of the atrium divided by the floor perimeter, as characteristic length scale. Note that one could also use the atrium height or width for the scaling.

The grid consists of 43200 cubic cells in the adjacent room and 518400 cells of the same size (2.5 cm and 20 cm edge in respectively small and large-scale simulations) in the atrium. A grid refinement study has been performed with finer grids, revealing no change in smoke layer height results or temperature fields.

In scaling the configurations, we want to keep the temperature field identical to that in the original simulation. As temperatures remain practically identical, c_p values and densities also remain unchanged. Gravity and initial molecular dynamic viscosity can be varied on purpose in the simulations (see below).

At the smoke outlet in the centre of the ceiling, a constant velocity u_{out} is imposed over the entire surface of the outlet opening. The walls of the atrium are adiabatic. As conductive and convective heat transfer scale in different ways in the program [9], it is inherently impossible to attain proper scaling with non-adiabatic walls. With this choice comes also the necessity to exclude radiation modeling. The convective heat release rate is imposed in the simulations, assuming a radiative loss of 35%.

The turbulent Schmidt and Prandtl numbers are kept constant.

From the Froude number (Eq. 5), it can be derived that the outlet velocity scales as

$$u_{out} \sim \sqrt{gD_h} \tag{22}$$

The Reynolds number (Eq. 6) provides the scaling for dynamic viscosity:

$$\mu \sim u_{out} D_h \tag{23}$$

The equivalency of velocity (Eq. 11) leads to the proper scaling law for the heat release rate of the fire:

$$\dot{Q} \sim u_{out} D_h^2 \tag{24}$$

Simulations

Six simulations were performed for this paper. Table 1 summarises the dimensionless numbers. In Table 1, the Re, Ra and Fr numbers are listed for the six simulations. The outlet velocity in the atrium was used to calculate these dimensionless numbers, with D_h as length scale. The numbers show that the flow is turbulent (Re > 10^4 and Ra > 10^9) in the simulations. Table 2 shows the parameter variations. The “basic” simulation (1) is based on one of the experiments of [8]. The imposed values are

presented in Table 3. In simulation 2, only the initial molecular viscosity is modified. As Reynolds and Rayleigh numbers are high, the flow is sufficiently turbulent, and changing the molecular viscosity should have no effect on the result. Note that in simulation 2, the Re and Ra numbers are not preserved with respect to simulation 1.

In simulation 3, the small atrium is again simulated, but the gravity has now changed. With Eqs. 22 through 24, the other initial parameters (Table 2) can be calculated to ensure that all three numbers Re, Ra and Fr are preserved. Although a simulation of this kind is not of great importance for practical problems that are 'sufficiently turbulent' (as is the case here, see below), it is interesting to show how scaling works when conserving all three numbers. Changing gravity in an experimental setup is very difficult, but can easily be done in CFD.

In simulation 4, the atrium is scaled up to a large-scale configuration. Only the Fr number of simulation 1 is preserved. Standard values are taken for gravity and molecular viscosity.

Simulation 5 of the large-scale atrium is scaled up from simulation 1, preserving Fr and Re. With respect to simulation 4, only the initial molecular viscosity is different.

The large atrium is again simulated in the simulation 6, but gravity has changed. Re, Ra and Fr are preserved.

Sim. n^o	**Re**	**$10^{-4}\cdot$ Re**	**Ra**	**$10^{-9}\cdot$ Ra**	**Fr**	**Fr**
1	Re_1	2.6	Ra_1	4	Fr_1	0.089
2	$a^{3/2}\,\mathrm{Re}_1$	60.0	$a^{3/2}\,\mathrm{Ra}_1$	2000	Fr_1	0.089
3	Re_1	2.6	Ra_1	4	Fr_1	0.089
4	$a^{3/2}\,\mathrm{Re}_1$	60.0	$a^{3/2}\,\mathrm{Ra}_1$	2000	Fr_1	0.089
5	Re_1	2.6	Ra_1	4	Fr_1	0.089
6	Re_1	2.6	Ra_1	4	Fr_1	0.089

Table 1. Important dimensionless numbers in the simulations. Symbol *a* represents the scaling factor, subscript 1 refers to values in simulation 1.

Sim.	***a***	$\dot{Q}$	μ	u_{out}	g	D_h	t
1		$\dot{Q}_1$	μ_1	u_1	g_1	$D_{h,1}$	t_1
2	8	$\dot{Q}_1$	$a^{-3/2}\,\mu_1$	u_1	g_1	$D_{h,1}$	t_1
3	8	$a^{-1/2}\,\dot{Q}_1$	$a^{-1/2}\,\mu_1$	$a^{-1/2}\,u_1$	$a^{-1}\,g_1$	$D_{h,1}$	$a^{1/2}t_1$
4	8	$a^{5/2}\,\dot{Q}_1$	μ_1	$a^{1/2}\,u_1$	g_1	$a\,D_{h,1}$	$a^{1/2}t_1$
5	8	$a^{5/2}\,\dot{Q}_1$	$a^{3/2}\,\mu_1$	$a^{1/2}\,u_1$	g_1	$a\,D_{h,1}$	$a^{1/2}t_1$
6	8	$a^{2}\,\dot{Q}_1$	$a\,\mu_1$	u_1	$a^{-1}\,g_1$	$a\,D_{h,1}$	at_1

Table 2. Scaling of the imposed parameters in the six simulations.

$\dot{Q}_1$	μ_1	$u_{out,1}$	g_1	W_1	H_1	$D_{h,1}$
kW	kg/sm	m/s	m/s^2	m	m	m
8.27	$18 \cdot 10^{-6}$	0.32	9.81	0.9	3.6	1.32

Table 3. Initial values of the imposed parameters in the six simulations.

Figure 2 shows the temperature profiles in each of the six simulations on a vertical line (at equivalent distance from the right hand side opening) in the atrium. It clearly shows that temperatures obtained in the different simulations are very similar.

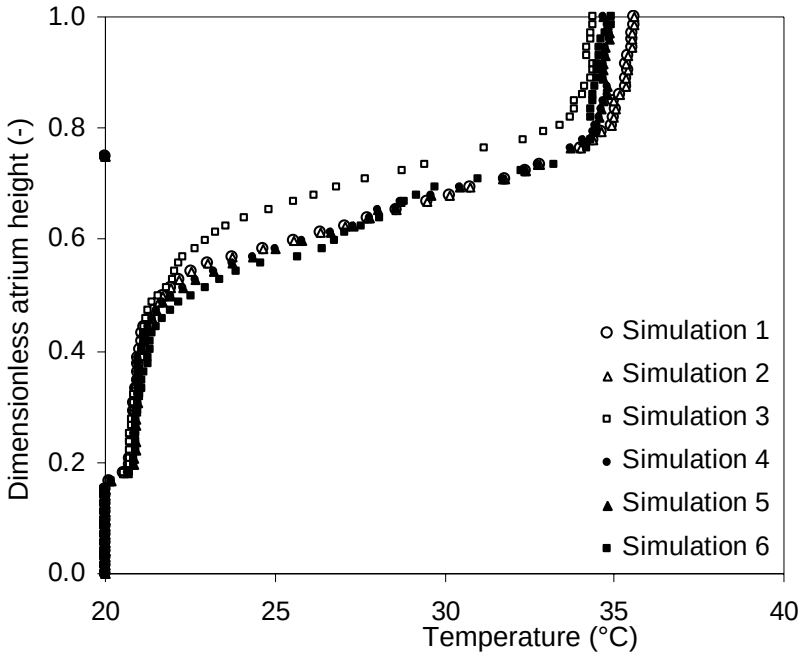

Figure 2. Temperatures on a vertical line (at dimensionless distance 0.94 from the adjacent room) in the simulations.

Discussion of the results

Figure 2 and 3 show that the temperature fields in the six simulations are in very good agreement with each other. This reveals that, for the test case under study, scaling up of the experiments based on the Froude number alone is allowed. This also means that the correlations, derived for small-scale setups, can be applied to larger scale configurations. We recall that this is most probably only true when all configurations are "sufficiently" turbulent.

This is clearly the case here. Indeed, when the only difference between two simulations is the initial molecular viscosity (1 vs. 2, and 4 vs. 5), the results are in very close agreement. This confirms the theoretical derivation that as long as the flow is sufficiently turbulent, molecular viscosity can be neglected with respect to the turbulent viscosity.

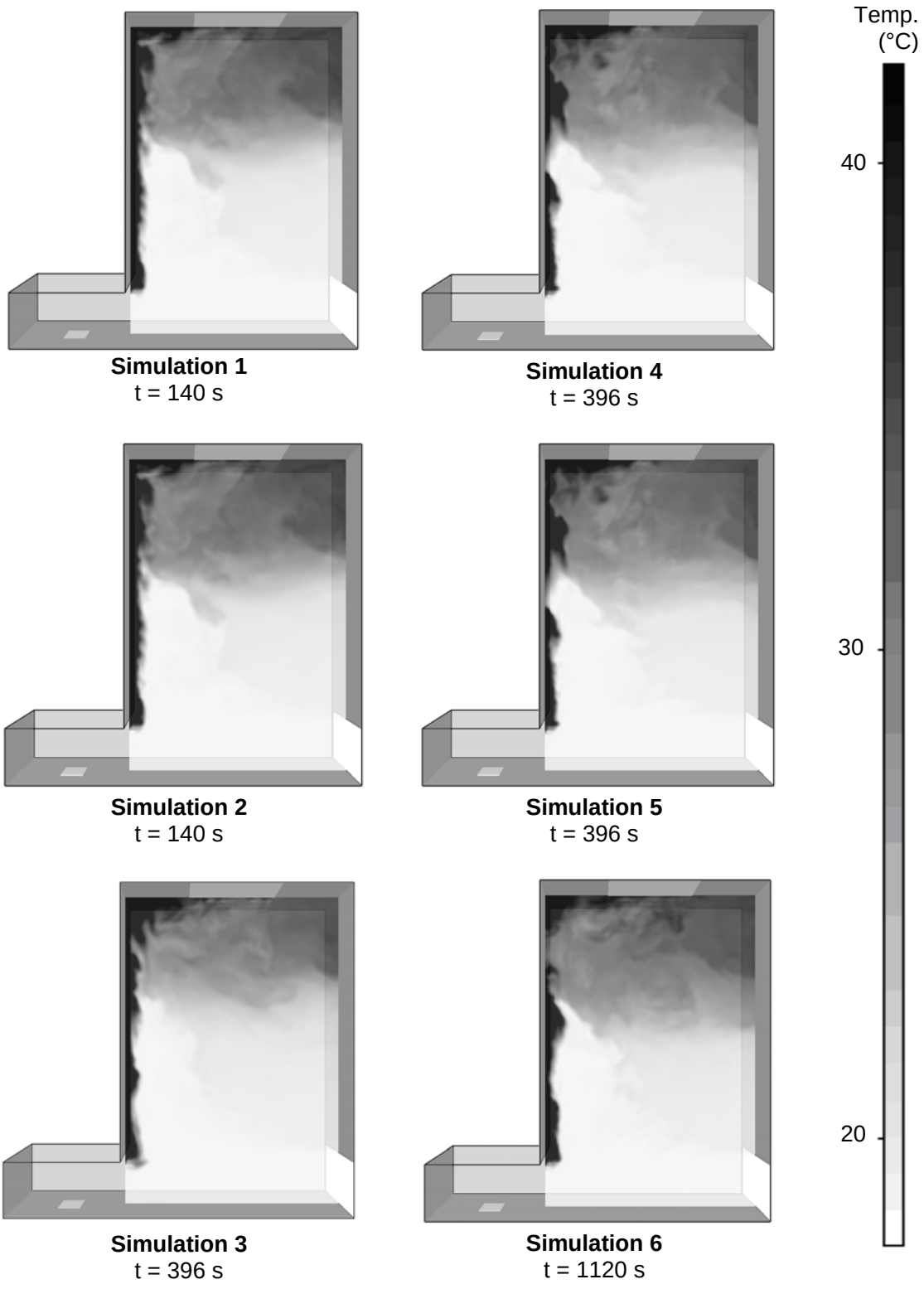

Figure 3. Temperature fields at corresponding time steps of the six performed simulations. Snapshots are taken at ‘equivalent scaled simulation times’, after a quasi steady-state smoke layer was obtained.

CONCLUSION

Scaling of setups was discussed, based on dimensionless numbers. In particular, CFD simulation results were discussed with LES to model turbulence. Scaling based on the Froude number only, seems allowed as long as all configurations are sufficiently turbulent. When using a Smagorinsky turbulence model, the turbulent Reynolds and Rayleigh numbers are indeed automatically preserved in scaling configurations by preserving the Froude number. Thus, as long as the flow is sufficiently turbulent, the effective Reynolds and Rayleigh numbers are automatically preserved and Froude scaling is allowed.

A number of CFD simulation results on an atrium configuration confirm this theoretical result. In future work, also configurations with lower Re and Ra numbers will be investigated.

ACKNOWLEDGEMENTS

Research funded by a Ph.D grant of the Institute for the Promotion of Innovation through Science and Technology in Flanders (IWT-Vlaanderen).

REFERENCES

1. Law, M., “A Note on Smoke Plumes from Fires in Multi-level Shopping Malls”, *Fire Safety Journal* 10(3): 197-202 (1986).
2. Thomas, P.H., “On the Upward Movement of Smoke and Related Shopping Mall Problems”, *Fire Safety Journal* 12(3): 191-203 (1987).
3. Law, M., “Measurements of Balcony Smoke Flow”, *Fire Safety Journal* 24(2): 189-195 (1995).
4. NFPA 92B, Smoke Management Systems in Malls, Atria and Large Areas, 2000 Edition, Publication No. 92B, National Fire Protection Association (2005).
5. Poreh, M., Morgan, H.P., Marshall, N.R., Harrison, R., “Entrainment by Two-Dimensional Spill Plumes”, *Fire Safety Journal* 30(1): 1-19 (1998).
6. Thomas, P.H., Morgan, H.P., Marshall, N., “The Spill Plume in Smoke Control Design”, *Fire Safety Journal* 30(1): 21-46 (1998).
7. Harrison, R., Spearpoint, M., “Entrainment of air into a balcony spill plume”, *Journal of Fire Protection Engineering* 16: 211-245 (2006).
8. Poreh, M., Marshall, N.R., Regev, A., “Entrainment by adhered two-dimensional plumes”, *Fire Safety Journal* 43: 344-350 (2008).
9. McGrattan, K., Klein, B., Hostikka, S., Floyd, J., Fire Dynamics Simulator (Ver.5) User’s Guide, NIST 1019-5, National Institute of Standards and Technology (2008).

10. Thomas, P.H. et. al., “Investigations into the Flow of Hot Gases in Roof Venting”, HMSO Fire Technical Paper No. 7 (1963)

11. Quintiere, J., *Fundamentals of Fire Phenomena*, John Wiley and Sons, Chichester, 2006.

12. Kumar, S., Thomas, P.H., Cox, G., “Novel Analytical Approach for Characterising Air Entrainment into a Balcony Spill Plume”, *Fire Safety Science* 9: 739-750 (2009)

13. Merci, B., Theuns, E., Sette, B., Vandevelde, P., “Numerical investigation of the error on flow measurements due to exhaust gas heating and cooling in the SBI-configuration”, *Fire And Materials* 31(1): 13-26 (2007)

14. Morgan, H.P., Ghosh, B.K., Garrad, G., Pamlitschka, R., De Smedt, J-C., Schoonbaert, L.R., “Design methodologies for smoke and heat exhaust ventilation”, BR368 Building Research Establishment, Garston, Watford, UK, (1999).